Aquat Geochem (2014) 20:419–435
DOI 10.1007/s10498-014-9227-x

ORIGINAL PAPER

The Importance of Microbial Iron Sulfide Oxidation for Nitrate Depletion in Anoxic Danish Sediments

Sarka Vaclavkova · Christian Juncher Jørgensen · Ole Stig Jacobsen · Jens Aamand · Bo Elberling

Received: 30 October 2013 / Accepted: 19 February 2014 / Published online: 7 March 2014

Abstract Nitrate (NO_3^-) reduction processes are important for depleting the NO_3^- load from agricultural source areas before the discharge water reaches surface waters or groundwater aquifers. In this study, we experimentally demonstrate the co-occurrence of microbial iron sulfide oxidation by NO_3^- (MISON) and other NO_3^--depleting processes in a range of contrasting sediment types: sandy groundwater aquifer, non-managed minerotrophic freshwater peat and two brackish muddy sediments. Approximately 1/3 of the net NO_3^- reduction was caused by MISON in three of the four environments despite the presence of organic carbon in the sediment. An apparent salinity limitation to MISON was observed in the most brackish environment. Addition of high surface area synthetically precipitated iron sulfide (FeS_x) to the aquifer sediment with the lowest natural FeS_x reactivity increased both the relative fraction of NO_3^- reduction linked to MISON from approximately 30–100 % and the absolute rates by a factor of 17, showing that the potential for MISON-related NO_3^- reduction is environmentally significant and rate limited by the availability of reactive FeS_x.

Keywords Microbial denitrification · Nitrate · Iron sulfide · Anoxic pyrite oxidation · Specific surface area · Freshwater and brackish environments

1 Introduction

Aquatic environments such as freshwater wetlands and wet meadows, brackish marshes, tidal environments and aquifers are potential buffers for counteracting excess loss of

S. Vaclavkova · C. J. Jørgensen · B. Elberling (✉)
Department of Geosciences and Natural Resource Management, University of Copenhagen, Øster Voldgade 10, 1350 Copenhagen K, Denmark
e-mail: be@ign.ku.dk

S. Vaclavkova · O. S. Jacobsen · J. Aamand
Department of Geochemistry, Geological Survey of Denmark and Greenland (GEUS), Øster Voldgade 10, 1350 Copenhagen K, Denmark

agricultural nitrogen to the aquatic environments. In these environments, agricultural nitrate (NO_3^-) is typically reduced to nitrogen gas (N_2) using organic carbon as an electron donor in the process of heterotrophic denitrification (HD) (Tiedje et al. 1982). The presence of iron sulfides (FeS_x) is a common feature for these shallow aquatic environments characterized by high organic carbon contents and moderate-to-high sulfate (SO_4^{2-}) availability (Canfield et al. 1993). Different reduced sulfur compounds including FeS_x have recently been shown to function as alternative electron donors for NO_3^- reduction in a variety of anoxic environments. Burgin et al. (2012) documented microbial NO_3^- reduction by dissolved hydrogen sulfide (H_2S) in entropic lakes, Schippers and Jørgensen (2002) suggested iron sulfide (FeS) to be a possible electron donor in marine sediments and (Jørgensen et al. 2009) documented NO_3^- coupled to pyrite (FeS_2) oxidation in carbon-poor aquifer sediment.

In this study, NO_3^- reduction in four FeS_x-rich environments is studied in a number of incubation experiments. In the sediment from these natural environments, reduced FeS_x occurs in variety of elemental and mineralogical compositions, reflecting the chemical bonding, crystallographic properties and ratio of ferrous iron (Fe^{2+}) to reduced sulfide (S^-) in the range between FeS and FeS_2. Depending on its overall reactivity, FeS_x has the ability to serve as electron donor in NO_3^- reduction processes (Brunet & Garcia-Gil 1996; Devlin et al. 2000; Rivett et al. 2008; Miotliński 2008; Jørgensen et al. 2009; Torrentó et al. 2010; Hayakawa et al. 2013) by the process of microbial iron sulfide oxidation by nitrate (MISON) producing SO_4^{2-} as the terminal product of FeS_x oxidation (see Eqs. 1–2). :

$$\text{Iron mono-sulfide (FeS)}: 5FeS + 8NO_3^- + 8H^+ \Rightarrow 4N_2 + 5Fe^{2+} + 5SO_4^{2-} + 4H_2O \quad (1)$$

$$\text{Iron di-sulfide (FeS}_2\text{)}: 5FeS_2 + 14NO_3^- + 4H^+ \Rightarrow 7N_2 + 10SO_4^{2-} + 5Fe^{2+} + 2H_2O \quad (2)$$

Although the co-occurrence of the two potential electron donors for NO_3^- reduction, organic carbon and reactive FeS_x, is common in nature, the relative proportion of co-occurring NO_3^- reduction by MISON and other NO_3^--depleting processes such as HD or NO_3^- assimilation remain unexplored.

We hypothesize that MISON can co-occur as a NO_3^--depleting process in a number of environments relevant for lowering agricultural nitrogen losses to the environments and could be non-competitive with other NO_3^--depleting processes as long as substrate availability of NO_3^- (i.e., NO_3^- concentration) and reactive surface area of FeS_x [i.e., specific surface area (SSA)] are not limiting factors.

2 Materials and Methods

The hypothesis is tested on the basis of a number of anaerobic incubation experiments with four diverse, iron sulfide (FeS_x)-rich sediment types from a shallow groundwater aquifer situated under an agricultural field, a non-managed minerotrophic freshwater wetland and two brackish sites, where agricultural stream water is discharged into shallow coastal areas with more or less saline conditions. Measured sulfate (SO_4^{2-}) production rates are used to quantify the molar ratio of nitrate (NO_3^-) reduction coupled to MISON, whereas NO_3^- reduction rates are used as a measure for total NO_3^- depletion (i.e., the sum of HD, NO_3^- assimilation and MISON-related NO_3^- reduction).

2.1 Study Sites and Sediment

Sediment samples used in the incubation experiments represent four different environments—a shallow groundwater aquifer, a freshwater wetland and two brackish coastal sites—each representing a typical environment with co-occurring NO_3^-, labile organic carbon compounds and FeS_x. All four environments thereby constitute areas with a potential for in situ reduction in excess NO_3^- loss to the aquatic environments and drinking water aquifer by both HD and MISON as well as sites with an increasing marine influence in terms of salinity.

Sediment samples representing typical shallow groundwater aquifer conditions were obtained from an unconfined sandy aquifer at Fladerne Bæk in Western Jutland, Denmark (56°17′ 29.06″N, 9°1′ 20.38″E). The upper parts of the aquifer (approximately 0–20 m) consist of quaternary melt water sand with reworked Miocene sediment of brackish and fresh water origin consisting of alternating layers of quarts sand, micaceous sand, silt and clay with sub-ordinate layers of lignite and secondary amorphous FeS_x (Rasmussen et al. 2007). The groundwater table is about 2–3 m below surface (mbs) and fluctuates seasonally by approximately 1.5 m (Jørgensen et al. 2009). Sediment from the Fladerne Bæk field site has previously been used to document that NO_3^- reduction by pyrite (FeS_2) oxidation is a microbial process (Jørgensen et al. 2009). Depth-specific sampling of the aquifer sediment was performed according to Jørgensen et al. (2009) using sand bailer.

Organic-rich wetland sediment was sampled in Maglemosen, which is a temperate freshwater wetland near Vedbæk, 20 km north of Copenhagen, Denmark (55°56′0.97″N, 12°31′18.22″E). The wetland was formed through the retreat of an ancient inlet, which subsequently turned into a lake and finally a wetland. The thickness of the peat is 0.5–3 m and the water level fluctuates from ground level to 0.7 cm below the surface (Jørgensen et al. 2012). The study site has not been managed for over a hundred years and is dominated by graminoids and different herbs (Elberling et al. 2011). Sediment samples were collected using a soil auger from a depth of 1.0 m below the surface.

Brackish sediment samples were collected near the coast at two different sites on Zealand, Denmark; coastal marsh of the east Zealand coast, Nivå (55°56′ 0.97″N, 12°31′ 18.22″E) and North-East side of Roskilde fjord (55°54′ 3.68″N, 12°2′ 41.97″E).

Nivå coast, about 32 km North of Copenhagen, is an East-facing low-energy coast partly protected by a barrier coast in its early stage. The coast is flat, and sediments are characterized by relatively fine-grained sediment. The site selected for sampling is the most protected and muddy part of the coast with mean water depth of 0.3 m, a conductivity of 13,200 μS cm^{-1} (moderately brackish) and no vegetation. Sediment was collected 0.6–0.7 m below the sediment surface using a spade.

Roskilde fjord is a shallow estuary covering an area of 122 km^2 and connected to Kattegat to the North. The site selected for sampling is the more protected Eastern coast where the sediment is mainly muddy. Fresh water discharge of Roskilde fjord is 350×10^6 m^3 per year (Flindt et al. 1997). The mean water depth at the sampling site is 0.4 m with conductivity of 25,200 μS cm^{-1} (heavily brackish), and the sampling site is free of vegetation. Sediment was collected 0.4–0.5 m below sediment surface using a spade.

To avoid contact with atmospheric oxygen, the water-saturated sediments were sealed in airtight glass jars immediately after retrieval and stored at 5 °C until incubation.

Mean annual air temperature is approximately 8 °C for all sites with mean annual precipitation in the range from 600 to 800 mm (climate normal for 1961–1990, Danish Meteorological Institute).

2.2 Iron Sulfide

Two different types of FeS_x were prepared using the total surface area of the mineral (measured by BET) as proxy for overall reactivity (similar to Torrentó et al. 2010). Crushed and ground natural crystalline FeS_2 was used to simulate a iron sulfide type of lower reactivity, while a chemically prepared mixture of iron sulfides (FeS_x) was used to simulate natural secondary iron sulfides consisting primarily of highly reactive framboidal FeS_2 (Fig. 1).

Natural crystalline FeS_2 comes from the Nanisivik mine in Northern Canada (Elberling et al. 2003), and the elemental composition was analyzed by X-ray fluorescence. Chemically, it is pyrite with minor contribution of silicates and oxides such as SiO_2, CaO, K_2O and zinc minerals (Jørgensen et al. 2009). Pyrite crystals were crushed by a hammer, then by hand in a mortar and subsequently crushed for 20 min in a ball mill. Finally, the grain mixture was vibrated in brass sieves (45, 180 and 360 μm pores). Each fraction was then washed and ultrasonicated in milliQ water to remove microparticles adhering to pyrite surfaces. To avoid coating, each fraction was shaken for 1 h in 1 M hydrochloric acid, washed with milliQ water, suction dried and sterilized with ethanol 95 % and then left overnight in a glove box in nitrogen (96 %) hydrogen (4 %) atmosphere. In the glove box, the FeS_2 was packed and afterward kept in air-tight glass containers.

A synthetic FeS_x precipitate of FeS_2, mackinawite ($(Fe)_{1+x}S$ (where $x = 0$–0.11)) and greigite (Fe_3S_4) was produced by reaction in a bacteria-free liquid medium with Na_2S at anoxic conditions according to Gramp et al. (2010). This mixture of FeS_x minerals represents a range of iron sulfides that can be expected in anoxic natural sediment with continuous FeS_x production. Each of the 1 L bottles contained 30 g of $Na_2S \times 9H_2O$ i.e., 0.125 mol S, 5.0 g Na-citrate, 1.0 g NH_4Cl and 0.14 g KH_2PO_4. The bottles were flushed with N_2 (nitrogen grade 5.0). The initial pH in the bottles of approximately 13.2 was lowered to 7–8 by addition of sulfuric acid. Addition of 17.89 g of FeCl2 $\times$ $4H_2O$ (0.09 mol Fe2 +) caused a precipitation of FeS_x minerals that was washed in 96 % ethanol and dried in an anaerobic glove box prior to use. The surface characteristics, including surface area, were assessed using BET analysis (Micromeritics Gemini 2375, Nitrogen (Quality 5.0), evacuation rate and time: 150 mmHg min^{-1} for 5 min, samples dried for at least 24 h under vacuum at room temperature, Particle Analytical ApS, Denmark), and scanning electron microscopy (SEM) was performed for both the natural FeS_2 and the chemical synthesized FeS_x.

The SSA of the crushed natural crystalline FeS_2 fractions was 0.02 and 0.4 $m^2\ g^{-1}$, respectively, whereas the SSA of the chemically produced FeS_x was 8.3 $m^2\ g^{-1}$. SEM pictures of the FeS_x powder show differences in the surface structure of the FeS_x with clear crystals of natural FeS_2 and porous particles of chemically precipitated FeS_x (Fig. 1c).

2.3 Incubation Experiments

Reactors were assembled adding 100 ± 1.00 g water-saturated sediment, 472.5–485 mL Milli-Q water and KNO_3 solution to 585 mL glass bottles that subsequently were closed with a chlorobutyl rubber septa and aluminum crimp (see Jørgensen et al. 2009 for further details). KNO_3 solution was added to reach NO_3^- concentrations of 5–50 mg L^{-1}, where the upper tested concentration is the limit of NO_3^- allowed in drinking water sources and aquatic environment by European Commission (ECEU 2008; ECEU 2009) and also represents realistic concentration leaching into the subsurface aquatic environments, where concentrations up to 300 mg L^{-1} were documented (Jacobsen et al. 1990; Postma et al.

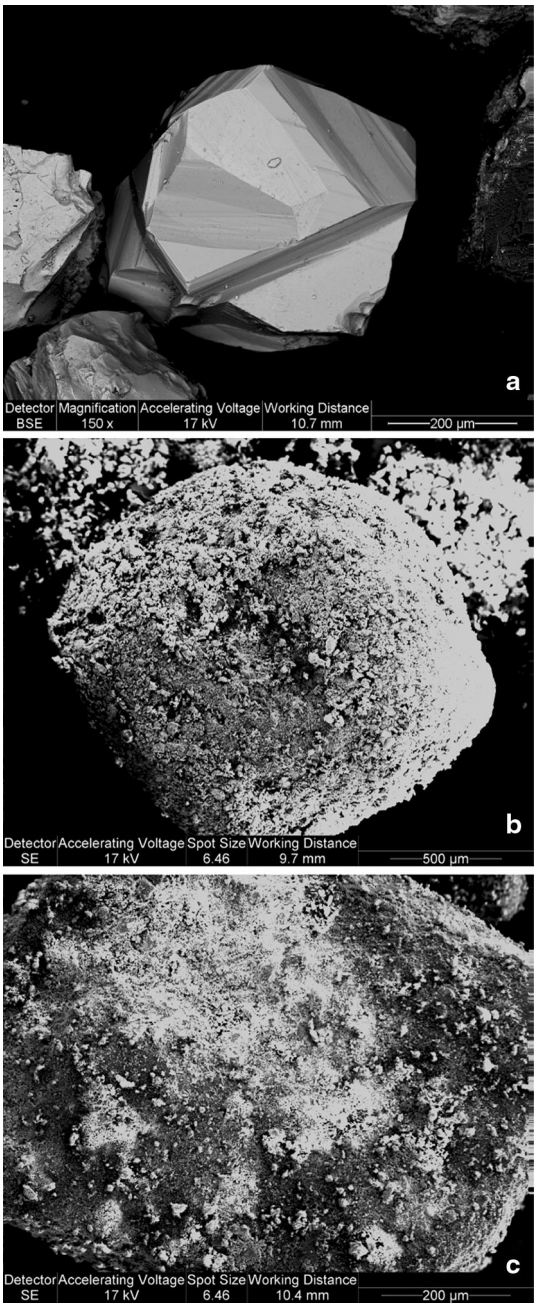

Fig. 1 Scanning electron microscope (SEM) images of the three different iron sulfide FeS_x fractions used in the incubation experiments: **a** crystalline pyrite (FeS_2) with a SSA of 0.02 $m^2\ g^{-1}$, **b** crystalline pyrite (FeS_2) with a SSA of 0.40 $m^2\ g^{-1}$, **c** synthetically precipitated iron sulfide (FeS_x) with a SSA of 8.30 $m^2\ g^{-1}$

1991; Bottrell et al. 2000; Pauwels et al. 2010). For the FeS_x amendment experiments, 1 ± 0.02 g FeS_2 was added to the solution and mixed mechanically by shaking the reactors. To achieve sterile initial conditions, all bottles, cups, needles, septa and solutions were autoclaved at 121 °C for 30 min prior to use. Abiotic control reactors were prepared

with sediment treated with either gamma irradiation with 25 kGy (Risø High Dose Reference Laboratory, DTU Denmark) or repeated autoclaving at 121 °C under 1.4 bars for 30 min. Autoclave sterilization was repeated 3 times at 24-h intervals.

To provide completely anaerobic conditions, all ingredients were added to the reactors under a flow of nitrogen (nitrogen grade 5.0 passing through a reactive copper column). To be sure that all residual oxygen was removed, the solution and headspace was flushed and over-pressured further by nitrogen for another 15 min using two sterilized stainless steel needles (TERUMO 18G, 1.2 × 40 mm and 17G 1.2 × 150 mm) temporary penetrating the septum. Oxic control reactors followed the same set-up as anoxic reactors after which short stainless steel needle was fastened permanently through the septum. All reactors were prepared in triplicate and incubated in dark at room temperature (20 °C). Each reactor was over-pressured by 25 mL of nitrogen with a sterile disposable syringe and needle prior to each sampling, where a 15 mL solution sample was extracted.

Reactors with natural sediment and with sterilized sediment from all four sampling sites were prepared. Aquifer sediment was further used in reactors amended with crystalline pyrite with SSA of 0.02 and 0.4 $m^2\ g^{-1}$, reactors amended with FeS_x mixture with SSA of 8.3 $m^2 g^{-1}$ and oxic reactors.

2.4 Chemical Analysis

Water samples were extracted from the reactors according to Jørgensen et al. (2009). Sediment samples were analyzed for total contents of nitrogen, carbon and sulfur by combustion in a LECO CS-200 oven. FeS_2 content of the natural sediment was determined by two-step extraction. In the first step, sediment was boiled in 20 % hydrochloric acid for 4 h to remove all non-pyrite-associated iron and sulfide. This was followed by boiling the washed sediment in concentrated nitric acid for 16 h, releasing pyrite-associated iron and sulfide to solution (Huerta-Diaz and Morse 1992). Pyrite-associated iron was determined spectrophotometrically (Jenway 6405 Spectrophotometer) by reaction with bipyridine and recalculated to soil FeS_2 content assuming a typical FeS_2 molar ratio of $\approx$1:2.

Electrical conductivity of the in situ water samples was measured by inserting the probes directly into fully water-saturated soil (Mettler Toledo FE30 with LE 703 Conductivity electrode).

All water samples were analyzed for pH using a Mettler Toledo (MP220 with Inlab 410 electrolyte 9823), and total alkalinity was determined by titration of 10 mL solution with 0.02 M hydrochloric acid (Schott Titroline easy with L300 electrolyte) to an end-point of pH 4.2 and with a precision better than 5 % and a detection limit equal to 0.005 $meqL^{-1}$. The concentration of free ferrous iron in solution was measured spectrophotometrically (Jenway 6405 Spectrophotometer) by reaction with bipyridine acetal buffer reagent at 520 nm according to Jørgensen et al. (2009) with a precision on average better than 5 % and a detection limit of 0.1 mg L^{-1}. Concentrations of NO_3^-, NO_2^- and SO_4^{2-} were measured within 24 h after sampling by ion chromatography (Dionex Ionpac AS14 4 mm column, CD20 conductivity detector and GP50 gradient pump) with a precision on average better than 2 % and a detection limit of 0.1 mg L^{-1}.

2.5 Data Analysis

The accumulated amount of moles n (NO_3^- and SO_4^{2-}) of element i removed from or released to the reactor solution over time up to sampling occasion k was calculated from the measured concentration (C_{meas}) according to Jørgensen et al. (2009):

$$n_i^k = \left[C_{i,\text{meas}}^k V_{\text{total}}^k + \sum_{s=1}^{k} C_{i,\text{meas}}^s V_{\text{sample}}^s \right] \text{(moles)} \quad (3)$$

where V_{total}^k is the total volume of solution in the reactor after removal of the kth sample and V_{sample}^s is the volume of sample removed on sampling occasion k. Elemental transformation rates were calculated using linear regression with time as independent variable and concentration as dependent variable. Average reaction rates are expressed as μmol per 100 g^{-1} sediment day^{-1} with the standard error of the mean value (±SE).

The rate effect of the initial NO_3^- concentrations on NO_3^- depletion rates and SO_4^{2-} production rates was evaluated by analysis of variance (one-way ANOVA). As a default, significance level value $p = 0.05$ was chosen and null hypothesis (H_0), stating that mean rate values of NO_3^- reduction or SO_4^{2-} production between the different sediment types are equal.

2.6 Calculation of the Observed NO_3^- Depletion Explained by FeS_x Oxidation

The total observed NO_3^- depletion reflects the net sum of NO_3^- reduction by MISON and other NO_3^- depleting processes. The relative amount of the total measured NO_3^- depletion, which can be directly ascribed to MISON can be calculated based on the stoichiometric ratio between the NO_3^- reduction and SO_4^{2-} production rates (Haaijer et al. 2007). Assuming that 8 mol of NO_3^- reduced by 5 mol of FeS would produce 5 mol of SO_4^{2-} and 14 mol of NO_3^- reduced by 5 mol FeS_2 would produce 10 mol of SO_4^{2-} (Jørgensen et al. 2009; Torrentó et al. 2010, Eqs. 1–2), the ideal NO_3^- to SO_4^{2-} ratio is 1.6 if all NO_3^- is reduced by FeS and 1.4 if all NO_3^- is reduced by FeS_2. By dividing the measured NO_3^- depletion rate ($a_{NO_3^-}$) with the measured SO_4^{2-} production rate ($a_{SO_4^{2-}}$), the deviation range from the ideal fractions can be calculated ($1.4–1.6/(a_{NO_3^-}/a_{SO_4^{2-}})$), which expresses the proportion (%) of observed NO_3^- reduction that can be explained by SO_4^{2-} production related to MISON. The remaining part of the observed NO_3^- depletion may be explained by a combination of other NO_3^- depleting processes, e.g., NO_3^- reduction by organic carbon, dissimilatory NO_3^- reduction to ammonium (NH_4^+), NO_3^- reduction by Fe^{2+} or NO_3^- uptake by microbes (Rivett et al. 2008).

3 Results

3.1 Sediment Characteristics

Characteristics of the four sediment types are shown in Table 1. Sediment pH was measured to be in the neutral range of 5.5 (sandy aquifer material) to 7.6 (brackish sediment). The wetland sediment consisting of decomposed peat had approximately 2–200 times higher % total C than the aquifer and brackish sediment and approximately 70–150 times higher % total N. The conductivities of the Fladerne Bæk (aquifer) and Maglemosen (wetland) sediment are in the freshwater range, whereas the Nivå and Roskilde Fjord are moderately to heavily brackish (compared to the conductivity of seawater ~54.000 μS cm^{-1}) (Leppäranta and Myrberg 2008). On a mass basis, most of the total % S was found in the FeS_2 fraction for all four environments, with the highest absolute concentrations being in the wetland sediment and the lowest concentration being in the brackish environments (Table 1).

Table 1 Natural sediment characteristics for the four environments

Locations sediment type	Fladerne Bæk freshwater aquifer	Maglemosen freshwater wetland	Nivå Moderately brackish	Roskilde heavily brackish
Sample depths (mbs)	11.0	1.0	0.6	0.4
pH	5.5	7.1	7.7	7.5
Conductivity ($\mu S\ cm^{-1}$)	355	1,214	13,200	25,200
% organic C	0.01	27.6	0.09	0.89
%N	0.02	2.07	0.03	0.01
%S	0.08	2.24	0.03	0.03
% FeS_2	0.06	2.30	0.03	0.03

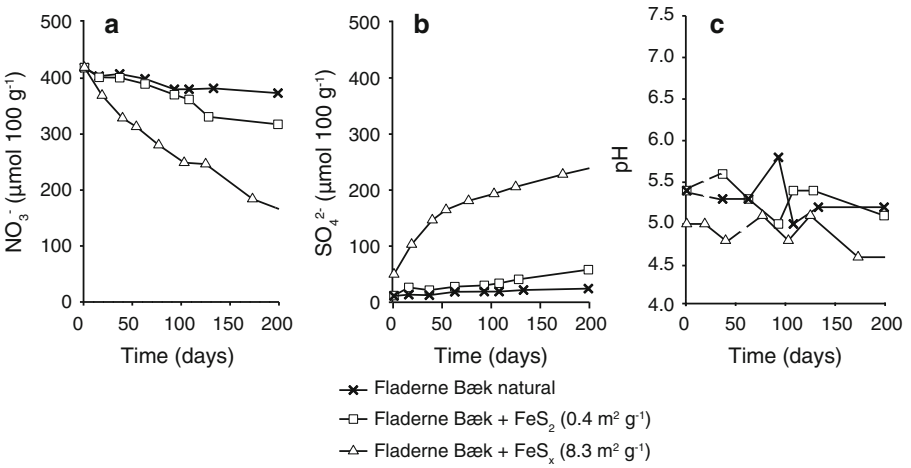

Fig. 2 Temporal trends of NO_3^- (**a**), SO_4^{2-} (**b**) and pH (**c**) in reactors with aquifer sediment with and without the addition of crystalline FeS_2 or synthetic FeS_x precipitate. The reactors were incubated at 22 °C for 199 days

3.2 Experimental NO_3^- Reduction by Anoxic FeS_x Oxidation

Temporal trends in NO_3^-, SO_4^{2-} and pH over 199 days in anoxic aquifer sediment are shown in Fig. 2. Trends are shown with and without the addition of crystalline FeS_2 (SSA: 0.4 $m^{-2}\ g^{-1}$) and synthetic FeS_x (SSA: 8.3 $m^{-2}\ g^{-1}$) at room temperature with an initial NO_3^- concentration of about 400 µmol NO_3^- per reactor ($\sim$50 mg L^{-1} NO_3^-). The variability between replicates ($n = 3$) is shown in Fig. 3. Decreasing NO_3^- concentrations over time was observed in all three treatments with the lowest rate being in the natural aquifer sediment and the highest rate being where the synthetic FeS_x was added (Fig. 2a). Increased concentrations of SO_4^{2-} were observed in all three treatments with the lowest rate being in the natural aquifer sediment and the highest rate being where synthetic FeS_x was added (Fig. 2b). pH levels in the three treatments were in the range of 4.5–6 with no significant development over time (Fig. 2c). Total alkalinity and total dissolved ferrous iron (Fe^{2+}) were below the detection limit in all three treatments (Fig. 3).

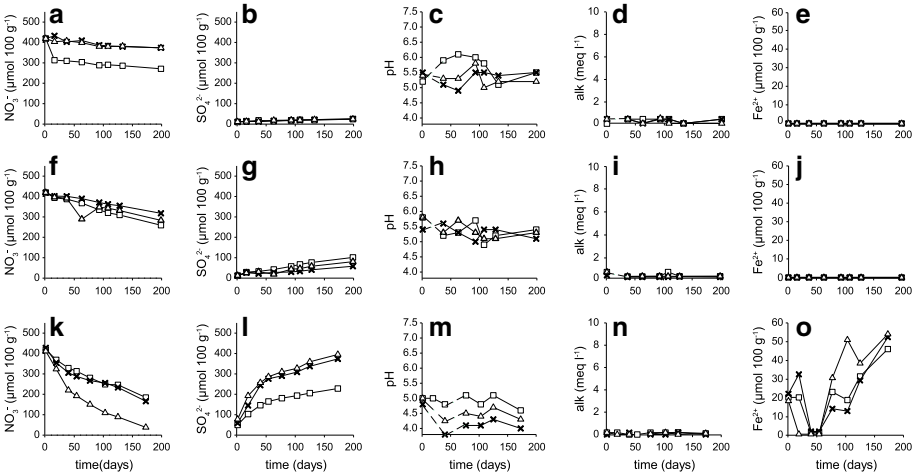

Fig. 3 Variability between replicates ($n = 3$) of aquifer sediment with different FeS_x additions: **a–e** represent aquifer sediment without added FeS_2; **f–j** represent aquifer sediment with 0.4 m^2 g^{-1} FeS_2 and **k–o** represent aquifer sediment with 8.3 m^2 g^{-1} FeS_2. Figures show changes in concentrations over 199 days for NO_3^-; SO_4^{2-}; pH; alkalinity and Fe^{2+} at 22 °C

Changes in NO_3^-, SO_4^{2-} and pH over 19 days in wetland (Maglemosen), moderately brackish (Nivå) and heavily brackish (Roskilde fjord) sediment are shown in Fig. 4, and the variability between replicates ($n = 3$) is shown in Fig. 5. Within the first 19 days of incubation, decreasing NO_3^- concentrations of up to 85 % of the initial concentrations were observed for all three environments (Fig. 4a). Concentrations of SO_4^{2-} were observed to increase in all three environments from initial concentrations reflecting the origin of the different environments (Fig. 4b). No significant change over time was observed for pH (Fig. 4c), alkalinity or Fe^{2+} (Fig. 5) in the brackish environments.

In the wetland sediment, the alkalinity increased by approximately 75 % over the first 8 days after incubation followed by a gradual decrease to a slightly elevated level compared to the initial alkalinity. The Fe^{2+} concentrations exhibited an initial fluctuation with an end concentration of approximately 50 % of the initial value (Fig. 5).

Complete inhibition of NO_3^- depletion and SO_4^{2-} production was achieved in the radiated and autoclaved abiotic anoxic controls from all sediment types (Fig. 6). Oxic control reactors were used to follow potential FeS_x oxidation and iron precipitation caused by oxygen contamination in FeS_2 amended reactors (data not shown). No significant NO_3^- depletion was observed in the oxic controls, while SO_4^{2-} concentrations exceeded 900 µmol SO_4^{2-} 100 g^{-1} of sediment after 180 days of incubation. In the same reactors, pH levels decreased to approximately pH 3 due to production of protons following the aerobic oxidation of the FeS_x.

3.3 NO_3^- Reduction Related to MISON

Table 2 shows the average NO_3^- depletion and SO_4^{2-} production rate estimates from the incubations of sediment from the wetland, aquifer, moderately brackish and heavily brackish environments. NO_3^- depletion rates were approximately 50–60 times higher in the sediment from the near-surface wetland soil and brackish environments compared to

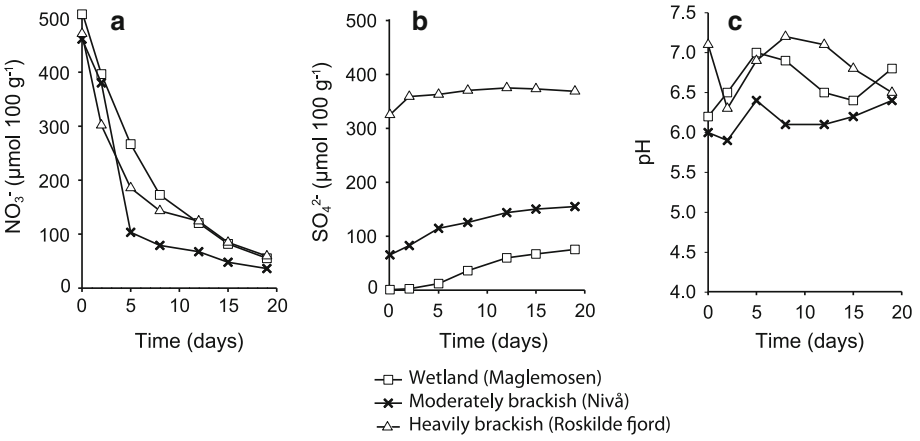

Fig. 4 Temporal trends of NO_3^- (**a**), SO_4^{2-} (**b**) and pH (**c**) in reactors with sediment from natural wetland and brackish environments incubated at 22 °C for 19 days

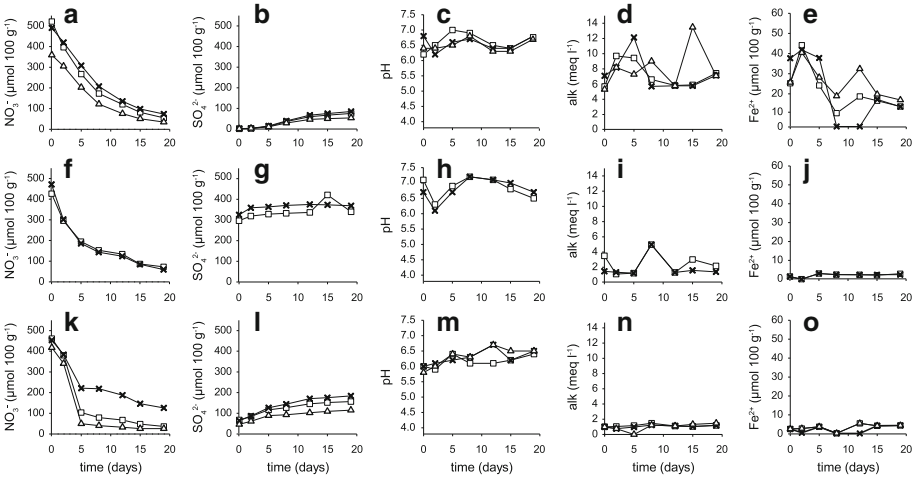

Fig. 5 Variability between replicates ($n = 3$) of wetland sediment (**a**–**e**), moderately brackish sediment (**f**–**j**) and heavily brackish sediment (**k**–**o**). Figures show changes in concentrations over 19 days for NO_3^-, SO_4^{2-}, pH, Fe^{2+} and alkalinity at 22 °C

the deeper aquifer sediment. With the exception of the heavily brackish sediment (Roskilde Fjord), significant SO_4^{2-} production rates were observed in all reactors with the lowest rates observed with the natural aquifers sediment and the highest rate with the wetland sediment. No significant difference was observed in SO_4^{2-} production rates between the wetland sediment and moderately brackish sediment ($p > 0.05$). In the reactors with heavily brackish sediment, SO_4^{2-} concentrations were stable over the incubation period with concentrations around 350 µmol 100 g^{-1} (Fig. 5). Addition of synthetic FeS_x (8.3 m^2 g^{-1}) to the aquifer increased reaction rates by approximately 7–17 times for NO_3^- depletion and SO_4^{2-} production rates, respectively (Table 2).

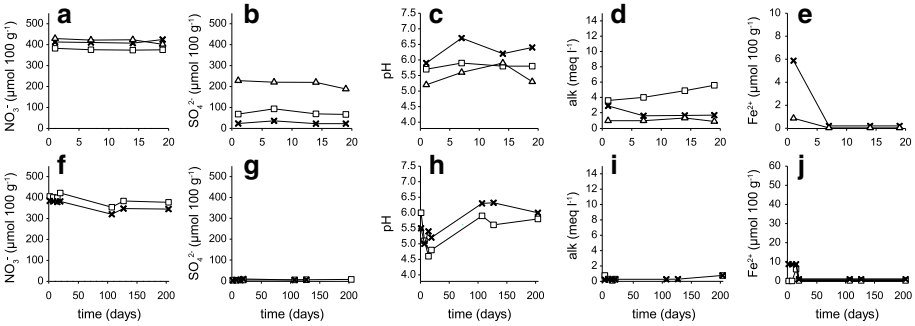

Fig. 6 Abiotic controls for contrasting environments (**a**–**e**): wetland sediment shown as *open squares*, moderately brackish shown as crosses and heavily brackish sediment shown as *open triangles* as well as abiotic controls after different treatment of aquifer sediment (**f**–**j**): radiated sediment shown as *open squares* and autoclaved sediment shown as crosses. Figures show changes in concentrations over 19 and 199 days for **a** NO_3^-, **b** SO_4^{2-}, **c** pH, **d** Fe^{2+} and **e** alkalinity at 22 °C

Table 2 NO_3^- depletion and SO_4^{2-} production rates and ratios as well as percentage of total NO_3^- reduction explained by microbial iron sulfide oxidation by nitrate (MISON-N) for the four environments

Sediment type	aNO_3^- (µmol 100 g^{-1} day^{-1})	aSO_4^{2-} (µmol 100 g^{-1} day^{-1})	aNO_3^-/aSO_4^{2-} ratio (N:S ratio)	MISON-N reduction (% range: FeS_2 to FeS)
Aquifer	0.23 ± 0.15	0.07 ± 0.00	4.7 ± 2.5	29.8 − 34.0
Aquifer + FeS_x	1.58 ± 0.66	1.18 ± 0.60	1.4 ± 0.1	100.0 − 114.3
Wetland	21.09 ± 3.19	4.33 ± 1.09	5.0 ± 0.7	28.0 − 32.0
Moderately brackish	18.77 ± 2.52	4.19 ± 1.46	4.2 ± 1.6	33.3 − 38.1
Heavily brackish	17.46 ± 1.39	Non significant	–	0

The absolute amount of NO_3^- that can potentially be reduced by MISON per mole FeS_x will vary according to the Fe to S ratio in the FeS_x, ranging from 1:1 in FeS to 1:2 in FeS_2 (see equations 1-2).The variation in the average percentage of the observed NO_3^- reduction, which can be explained by MISON differs slightly depending on the FeS to FeS_2 range from approximately 30–100 % (Table 2). In the aquifer, wetland and the moderately brackish sediment, MISON accounted for approximately 1/3 of the observed NO_3^- depletion. In the heavily brackish sediment, no significant SO_4^{2-} production was observed. In the treatment where synthetic FeS_x was added to the aquifer sediment, all of the observed NO_3^- depletion was accounted for by MISON-related SO_4^{2-} production. Variations in absolute SO_4^{2-} production rates were largest between the natural aquifer sediment and the wetland and moderately brackish environments. When synthetic FeS_x (8.3 m^2 g^{-1}) was added to the aquifer sediment SO_4^{2-} production rates increased from approximately 1.5–28 % of the wetland/moderately brackish (Table 2).

3.4 Effects of Specific Surface Area of FeS_x and NO_3^- Concentration

Results from the FeS_x reactivity experiment are shown in Fig. 7. No significant effect (1-way ANOVA) on NO_3^- depletion and SO_4^{2-} production rates was observed following

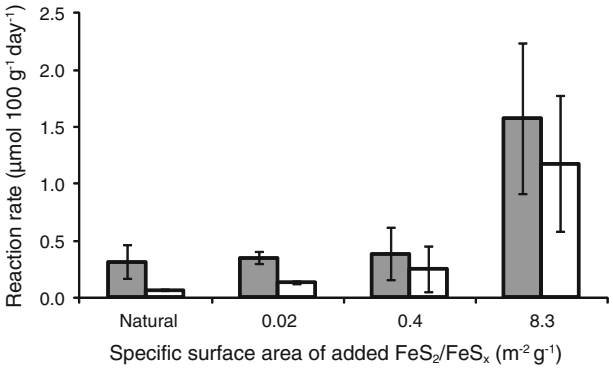

Fig. 7 Effect of FeS_2 addition (crystalline FeS_2 with SSA 0.02 and 0.4 m^2 g^{-1}) and synthetically precipitated FeS_x (SSA: 8.3 m^2 g^{-1}) on NO_3^- depletion and SO_4^{2-} production rates. *Gray columns*: NO_3^- and *white columns*: SO_4^{2-}

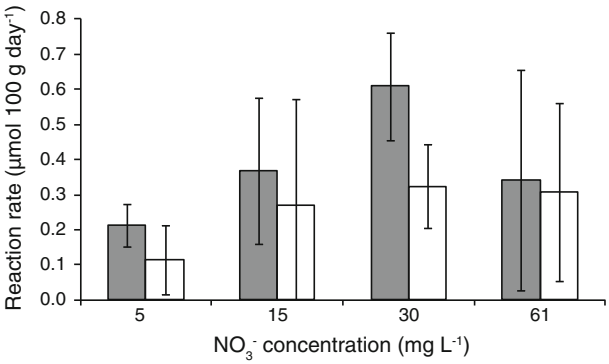

Fig. 8 Effect of initial NO_3^- concentration (aquifer sediment with 0.4 m^2 g^{-1} FeS_2 added) on NO_3^-depletion (*gray bars*) and SO_4^{2-} production rates (*white bars*)

addition of crystalline FeS_2 with SAA of 0.02 and 0.40 m^2 g^{-1} to the aquifer sediment. In contrast, NO_3^- depletion rates significantly increased by an average factor of 5 after the addition of synthetic FeS_x with a SSA of 8.30 m^2 g^{-1}. Significant increases in SO_4^{2-} production rates were observed in the treatment with synthetic FeS_x when compared to treatment using crystalline FeS_2 amended and non-amended natural aquifer sediment.

NO_3^- depletion and SO_4^{2-} production rates show no significant difference with respect to initial NO_3^- concentration in the concentration range of 5–50 mg NO_3^- L^{-1} in aquifer sediment amended with 0.40 m^2 g^{-1} FeS_2 (Fig. 8). Average SO_4^{2-} production rates were in the range of about 0.3 ± 0.04 µmol 100 g^{-1} day^{-1} independently of initial NO_3^- concentration. NO_3^- depletion rates have higher variation, with mean about 0.3–0.4 µmol 100 g^{-1} day^{-1}.

4 Discussion and Conclusions

While recent research has shown that microbial FeS_x oxidation by NO_3^- is an important microbial process in linking the interactions between the nitrogen (N) and sulfur (S) cycles (Jørgensen et al. 2009; Torrentó et al. 2010; Bosch and Meckenstock 2012; Hayakawa

et al. 2013), understanding of the process' potential impact on a broader environmental scale is lacking. HD is an important and widely documented ecosystem process responsible for the conversion of agricultural NO_3^- to atmospheric N_2 using soil organic matter (SOM) as electron donor. SOM, NO_3^- and reduced iron sulfur species commonly occur at a wide range of reduced environments including sediment systems both near the surface (Pons et al. 1982; Postma 1982; Folk 2005; Burgin et al. 2012) and in shallow groundwater aquifers (Rivett et al. 2008), and the potential co-occurrence of both HD and MISON under oxygen-free conditions seems therefore plausible as long as substrate availabilities or other environmental factors are non-limiting.

4.1 Evidence of Co-occurring NO_3^- Reduction by Iron Sulfide and Soil Organic Matter

Several processes can be involved in the net depletion of NO_3^- in submerged ecosystems (Rivett et al. 2008). HD is typically regarded as the most dominating N-depleting process in aquifer, wetland and brackish environments, being responsible for between 80 and 100 % of net NO_3^- depletion (Smith and Duff 1988; Laverman et al. 2006). In addition, MISON has been shown to be an important NO_3^--reducing process in aquifer environments (Frind et al. 1990; Korom et al. 2005; Jørgensen et al. 2009) where availability of organic carbon could be a rate limiting factor for HD.

This study shows that NO_3^- reduction and SO_4^{2-} production rates are linked directly to MISON in FeS- and FeS_2-containing sediment in the absence of dissolved oxygen (Figs. 2–5) since no other known S-source than FeS_x may facilitate the observed SO_4^{2-} production over time in the investigated freshwater and brackish sediment. In this way, estimates of the average percentage of the observed NO_3^- reduction, which can be explained by MISON, can be calculated based on a stoichiometric comparison of reactor specific NO_3^- depletion and SO_4^{2-} production rates (Table 2). The remaining part of the observed NO_3^- depletion may in this way be the product of HD, dissimilatory NO_3^- reduction to NH_4^+ and microbial N assimilation (Rivett et al. 2008). Despite the uncertainty of the relative proportions of ongoing non-MISON NO_3^- depleting processes, it is concluded that for both the natural aquifer, wetland and moderately brackish sediment, MISON-related NO_3^- reduction accounts for approximately 30 % of the total measured NO_3^- depletion despite the presence of organic carbon in all three sediment types (Table 1).

Addition of synthetic FeS_x (SSA: 8.30 $m^2\ g^{-1}$) to the aquifer sediment resulted in approximately 17 times higher SO_4^{2-} production rates than in the unamended sediment, indicating that MISON in this environment is substrate-limited (i.e., availability of FeS_x) rather than limited by microbial abundance (Table 1). Also, this addition increased the absolute SO_4^{2-} production rates to an order of 1/3 to the near-surface environments of the freshwater wetland and moderately brackish sediment. As far as we know, the SO_4^{2-} production rates directly related to MISON reported in this study are the highest reported to date and of a magnitude, which highlights the potential environmental importance of MISON for net NO_3^- depletion in a wide variety of environment where reduced FeS_x is present.

4.2 Evaluation of Potential Rate Limiting Factors: Specific Surface Area, Salinity, NO_3^- Concentration

The susceptibility of FeS_2 to oxidation depends on its microscopic structure and not all FeS_2 in a sediment may be available for the reaction (Schippers and Jørgensen 2001;

Haaijer et al. 2007; Rivett et al. 2008). The SSA is often used as proxy for the overall reactivity of FeS_2 in incubation studies (Jørgensen et al. 2009; Torrentó et al. 2010), knowing that the reactive surface area of a given FeS_2 under certain conditions can be significantly different than the total SSA (McKibben and Barnes 1986; Salmon and Malmström 2006).

Addition of crystalline FeS_2 in the 0.02 and 0.40 $m^2\ g^{-1}$ fraction to the aquifer sediment produced no significant stimulation ($p > 0.05$) of the NO_3^- depletion and SO_4^{2-} production rates compared to the reactors incubated with aquifer sediment with a natural FeS_2 content of 0.06 % (Fig. 7). A similar observation was made by Haaijer et al. 2007 where crystalline FeS_x did not function as electron donor for microbial NO_3^- reduction in a freshwater environment. However, significant SO_4^{2-} production ($p < 0.05$) due to MISON was observed in all natural and FeS_x amended reactors showing that the naturally occurring FeS_2 in the aquifer sediment is of reactive nature, possibly of secondary origin similar to the nearby field site investigated by (Postma et al. 1991).

Measured NO_3^- depletion and SO_4^{2-} production rates in the aquifer sediment were significant lower than in near-surface moderately brackish sediments. This study provides no evidence for these contrasting rates, but presence of nanosized framboidal FeS_2, and well as high microbial population density are known factors that can explain the higher rates observed in freshwater wetlands and brackish environments (Folk 2005; Postma 1982). Several interacting factors may limit rates in the aquifer sediment; a combination of low microbial population density and low substrate reactivity in the deeper aquifer sediment compared to the near-surface environments can be part of the explanation.

Significant increases in both NO_3^- depletion and SO_4^{2-} production rates were observed after the addition of synthetically precipitated FeS_x with an SSA of 8.3 $m^2\ g^{-1}$ (Fig. 7). The results showed that an increased availability of high surface area FeS_x substrate could stimulate the microbial consortia responsible for FeS_x oxidation by NO_3^- in the aquifer sediment in such a way that the percentage of NO_3^- depletion, which can be directly explained by MISON went from approximately 30–100 % (Table 2). This observation indicates that the presence of highly reactive FeS_x can produce increased NO_3^- reduction rates related to MISON in an environment where labile soil organic carbon is present. A comparison of total FeS_2 percentage in the sediment (Table 1) to MISON-related SO_4^{2-} production rates (Table 2) supports the observation that it is the overall reactivity of the FeS_x and susceptibility to oxidation which act as a rate limiting factor rather than the total amount of FeS_2 in the sediment. It is seen that SO_4^{2-} production rates in the moderately brackish environment are at levels similar to those of the wetland despite a significantly lower FeS_2 content and the fact that the aquifer sediment capacity to deplete NO_3^- can be drastically increased with the addition of high reactivity FeS_x (Table 2).

High salinity has been proposed as a potential inhibitor of denitrification in saline wastewater (Dincer and Kargi 1999; Ucisik and Henze 2004). However, relatively few studies have documented this potential inhibitory effect over a wider range of NO_3^- depleting environments (Kana et al. 1998; Magalhães et al. 2005). In the current study, we observed NO_3^- depletion in the two freshwater sediments and the brackish sediment (Tables 1 & 2) supporting the observations that HD and other NO_3^--depleting processes do not appear to be affected by the salinity levels found in estuarine and marine environments (Kana et al. 1998; Magalhães et al. 2005). The extent to which salinity controls the NO_3^- reduction coupled to MISON is still unknown. However, the observed absence of significant SO_4^{2-} production over time in the heavily brackish sediment suggests that an upper salinity limit (in this case between 13,200 and 25,200 μS cm^{-1}) might exist at which the microbial consortia involved in MISON may function.

Within the typical concentration range of NO_3^- in shallow aquifers and freshwater environment (5–50 mg L^{-1}), neither NO_3^- depletion rates nor SO_4^{2-} production rates were significantly rate limited by the effective NO_3^- concentration (Fig. 8), but decreasing trends for both NO_3^- depletion and SO_4^{2-} production rates were noted at low NO_3^- concentrations (5 mg L^{-1}). Similarly, Torrentó et al. (2010) described SO_4^{2-} production not to be limited by the effective NO_3^- concentration in range of 1–4 mM. Similar to other studies (Smith and Duff 1988; Korom et al. 2005; Rivett et al. 2008), we found that NO_3^- depletion rates could be described with zero-order kinetics (i.e., independent of concentration).

4.3 Environmental Implications

For future planning of agricultural N-buffer zones, increased understanding of the potential environmental effects of co-occurring MISON and other NO_3^--depleting processes is important for avoiding adverse effects on both the terrestrial and aquatic environments. If MISON is as an important process in addition to HD and other NO_3^--depleting processes in a wider range of near-surface and shallow environments as documented in this study, total nitrate-buffer capacities may be underestimated. Within the differences of sediment-specific reaction rates, MISON accounted for as much as 1/3 of the natural NO_3^- depletion in both aquifer and near-surface environments, showing that MISON can be an important NO_3^- depleting process in a range of freshwater and moderately brackish environments. Also, knowledge of the apparent salinity inhibition observed in the heavily brackish environment should be considered to improve predictions on the overall depletion of NO_3^- fluxes from land to marine ecosystems. While the presence of reactive FeS_x is a pre-requisite for MISON to occur, results show that it is the reactivity and mineralogical composition of the FeS_x that governs the potential NO_3^- reduction capacity related to MISON, rather than the absolute amount of FeS_x being present in the environment. Addition of crystalline FeS_2 to the aquifer sediment did not stimulate NO_3^- depletion or SO_4^{2-} production rates significantly, thereby indicating the overall rate limiting factors and boundary conditions for the potentially reactive FeS_x minerals. Nonetheless, when reactive FeS_x was present, consistent NO_3^- reductions, with MISON accounting for approximately 1/3 of the total NO_3^- reduction, were observed in all but the most saline environments despite the presence of labile organic carbon and NO_3^- depletion by HD and other NO_3^--depleting processes.

Acknowledgments This study was funded by a grant from Geocenter Denmark ("Geocenterbevilling MOPAG-project", Microbiol. GEUS: 05061 (PhD)) and received additional funding from the project "Nitrous oxide dynamics: The missing links between controls on subsurface N_2O production/consumption and net atmospheric emissions" financed by the Danish Natural Science Research Council and the Department of Geoscience and Natural Resource Management, University of Copenhagen, Denmark.

References

Bosch J, Meckenstock RU (2012) Rates and potential mechanism of anaerobic nitrate-dependent microbial pyrite oxidation. Biochem Soc Trans 40:1280–1283. doi:10.1042/BST20120102

Bottrell SH, Parkes RJ, Cragg BA, Raiswell R (2000) Isotopic evidence for anoxic pyrite oxidation and stimulation of bacterial sulphate reduction in marine sediments. J Geol Soc London 157:711–714

Brunet R, Garcia-Gil LJ (1996) Sulfide-induced dissimilatory nitrate reduction to ammonia in anaerobic freshwater sediments. FEMS Microbiol Ecol 21:131–138. doi:10.1016/0168-6496(96)00051-7

Burgin A, Hamilton S, Jones S, Lennon J (2012) Denitrification by sulfur-oxidizing bacteria in a eutrophic lake. Aquat Microb Ecol 66:283–293. doi:10.3354/ame01574

Canfield DE, Thamdrup B, Hansen JW (1993) The anaerobic degradation of organic matter in Danish coastal sediments: iron reduction, manganese reduction, and sulfate reduction. Geochim Cosmochim Acta 57:3867–3883

Devlin J, Eedy R, Butler B (2000) The effects of electron donor and granular iron on nitrate transformation rates in sediments from a municipal water supply aquifer. J Contam Hydrol 46:81–97. doi:10.1016/S0169-7722(00)00126-1

Dincer A, Kargi F (1999) Salt inhibition of nitrification and denitrification in saline wastewater. Environ Technol 20:1147–1153

Elberling B, Balić-Žunić T, Edsberg A (2003) Spatial variations and controls of acid mine drainage generation. Environ Geol 43:806–813. doi:10.1007/s00254-002-0695-8

Elberling B, Askaer L, Jørgensen CJ et al (2011) Linking soil O_2, CO_2, and CH_4 concentrations in a Wetland soil: implications for CO_2 and CH_4 fluxes. Environ Sci Technol 45:3393–3399. doi:10.1021/es103540k

Flindt MR, Kamp-Nielsen L, Marques JC et al (1997) Description of the three shallow estuaries : mondego River (Portugal), Roskilde Fjord (Denmark) and the Lagoon of Venice (Italy). Ecol Modell 102:17–31

Folk R (2005) Nannobacteria and the formation of framboidal pyrite: textural evidence. J Earth Syst Sci 114:369–374

Frind E, Duynisveld WH, Strebel O, Boettcher J (1990) Modelling of multicomponent transport with microbial transformation in groundwater: the Fuhrberg Case. Water Resour Res 26:1707–1719

Gramp JP, Bigham JM, Jones FS, Tuovinen OH (2010) Formation of Fe-sulfides in cultures of sulfate-reducing bacteria. J Hazard Mater 175:1062–1067. doi:10.1016/j.jhazmat.2009.10.119

Haaijer SCM, Lamers LPM, Smolders AJP, Jetten MSM, den Camp HJMO (2007) Iron sulfide and pyrite as potential electron donors for microbial nitrate reduction in freshwater wetlands. Geomicrobiol J 24:391–401. doi:10.1080/01490450701436489

Hayakawa A, Hatakeyama M, Asano R, Ishikawa Y, Hidaka S (2013) Nitrate reduction coupled with pyrite oxidation in the surface sediments of a sulfide-rich ecosystem. J Geophys Res Biogeosci 118:639–649. doi:10.1002/jgrg.20060

Huerta-Diaz M, Morse J (1992) Pyritization of trace metals in anoxic marine sediments. Geochim Cosmochim Acta 56:2681–2702

Jacobsen OS, Larsen HV, Andreasen L (1990) Nitrate recuction by pyrite and lignite in sandy aquifer. In: Nitrogen and phosphorus in soil and air—B-abstracts of the Danish Research Programme on Nitrogen Phosphorus and Organic Matter (NPo). 151–166

Jørgensen CJ, Jacobsen OS, Elberling B, Aamand J (2009) Microbial oxidation of pyrite coupled to nitrate reduction in anoxic groundwater sediment. Environ Sci Technol 43:4851–4857

Jørgensen CJ, Struwe S, Elberling B (2012) Temporal trends in N_2O flux dynamics in a Danish wetland - effects of plant-mediated gas transport of N_2O and O_2 following changes in water level and soil mineral-N availability. Glob Chang Biol 18:210–222. doi:10.1111/j.1365-2486.2011.02485.x

Kana TM, Sullivan MB, Cornwall JC, Groszkowski KM (1998) Denitrification in estuarine sediments determined by membrane inlet mass spectrometry. Limnol Oceanogr 43:334–339

Korom SF, Schlag AJ, Schuh WM, Kammer Schlag A (2005) In situ mesocosms: denitrification in the Elk Valley aquifer. Ground Water Monit Remediat 25:79–89. doi:10.1111/j.1745-6592.2005.0003.x

Laverman AM, Van Cappellen P, van Rotterdam-Los D et al (2006) Potential rates and pathways of microbial nitrate reduction in coastal sediments. FEMS Microbiol Ecol 58:179–192. doi:10.1111/j.1574-6941.2006.00155.x

Leppäranta M, Myrberg K (2008) Physical oceanography of the Baltic Sea. Springer, Berlin

Magalhães CM, Joye SB, Moreira RM et al (2005) Effect of salinity and inorganic nitrogen concentrations on nitrification and denitrification rates in intertidal sediments and rocky biofilms of the Douro River estuary, Portugal. Water Res 39:1783–1794. doi:10.1016/j.watres.2005.03.008

McKibben M, Barnes H (1986) Oxidation of pyrite in low temperature acidic solutions: rate laws and surface textures. Geochim Cosmochim Acta 50:1509–1520

Miotliński K (2008) Coupled reactive transport modeling of redox processes in a nitrate-polluted sandy aquifer. Aquat Geochem 14:117–131. doi:10.1007/s10498-008-9028-1

Pauwels H, Ayraud-Vergnaud V, Aquilina L, Molénat J (2010) The fate of nitrogen and sulfur in hard-rock aquifers as shown by sulfate-isotope tracing. Appl Geochem 25:105–115. doi:10.1016/j.apgeochem.2009.11.001

Pons L, van Breemen N, Driessen P (1982) Physiography of coastal sediments and development of potential soil acidity. In: Acid Sulphate Weathering, Part I. Soil Science Society of America, Madison, USA, pp 1–18

Postma D (1982) Pyrite and siderite formation in brackish and freshwater swamp sediments. Am J Sci 282:1151–1183
Postma D, Boesen C, Kristiansen H, Larsen F (1991) Nitrate reduction in an unconfined sandy aquifer: water chemistry, reduction processes, and geochemical modeling. Water Resour Res 27:2027–2045
Rasmussen ES, Vangkilde-Pedersen T, Scharling P (2007) Prediction of reservoir sand in miocene deltaic deposits in Denmark based on high-resolution seismic data. Geol Surv Den Greenl Bull 13:17–20
Rivett MO, Buss SR, Morgan P et al (2008) Nitrate attenuation in groundwater: a review of biogeochemical controlling processes. Water Res 42:4215–4232
Salmon SU, Malmström ME (2006) Quantification of mineral dissolution rates and applicability of rate laws: laboratory studies of mill tailings. Appl Geochem 21:269–288. doi:10.1016/j.apgeochem.2005.09.014
Schippers A, Jørgensen BB (2001) Oxidation of pyrite and iron sulfide by manganese dioxide in marine sediments. Geochim Cosmochim Acta 65:915–922
Schippers A, Jørgensen BB (2002) Biogeochemistry of pyrite and iron sulfide oxidation in marine sediments. Geochim Cosmochim Acta 66:85–92
Smith R, Duff J (1988) Denitrification in a sand and gravel aquifer. Appl Environ Microbiol 54:1071–1078
Tiedje JM, Sexstone AJ, Myrold DD, Robinson JA (1982) Denitrification: ecological niches, competition and survival. Antonie Van Leeuwenhoek 48:569–583
Torrentó C, Cama J, Urmeneta J et al (2010) Denitrification of groundwater with pyrite and *Thiobacillus denitrificans*. Chem Geol 278:80–91. doi:10.1016/j.chemgeo.2010.09.003
Ucisik AS, Henze M (2004) Biological denitrification of fertiliser wastewater at high chloride concentration. Watere SA 30:191–195